

1 Distinguish virulent and temperate phage-derived sequences in 2 metavirome data with a deep learning approach

3 Shufang Wu^{1,2}, Zhencheng Fang^{1,2}, Jie Tan^{1,2}, Mo Li³, Chunhui Wang³, Qian Guo^{1,2,4}, Congmin Xu^{1,2,4},
4 Xiaoqing Jiang^{1,2} and Huaqiu Zhu^{1,2,4,5*}

5 ¹ State Key Laboratory for Turbulence and Complex Systems and Department of Biomedical
6 Engineering, College of Engineering, Peking University, Beijing 100871, China

7 ² Center for Quantitative Biology, Peking University, Beijing 100871, China

8 ³ Peking University-Tsinghua University - National Institute of Biological Sciences (PTN) joint PhD
9 program, School of Life Sciences, Peking University, Beijing 100871, China

10 ⁴ Department of Biomedical Engineering, Georgia Institute of Technology and Emory University,
11 Georgia 30332, USA

12 ⁵ Institute of Medical Technology, Peking University Health Science Center, Beijing 100191, China.

13 * To whom correspondence should be addressed. Tel: 8610-6276 7261; Email: hqzhu@pku.edu.cn

14

15 **ABSTRACT**

16 Background: Prokaryotic viruses referred to as phages can be divided into virulent and temperate
17 phages. Distinguishing virulent and temperate phage-derived sequences in metavirome data is
18 important for their role in interactions with bacterial hosts and regulations of microbial communities.
19 However there is no experimental or computational approach to classify sequences of these two in
20 culture-independent metavirome effectively, we present a new computational method DeePhage,
21 which can directly and rapidly judge each read or contig as a virulent or temperate phage-derived
22 fragment.

23 Findings: DeePhage utilizes a “one-hot” encoding form to have an overall and detailed representation
24 of DNA sequences. Sequence signatures are detected via a deep learning algorithm, namely a
25 convolutional neural network to extract valuable local features. DeePhage makes better performance
26 than the most related method PHACTS. The accuracy of DeePhage on five-fold validation reach as
27 high as 88%, nearly 30% higher than PHACTS. Evaluation on real metavirome shows DeePhage
28 annotated 54.4% of reliable contigs while PHACTS annotated 44.5%. While running on the same

29 machine, DeePhage reduces computational time than PHACTS by 810 times. Besides, we proposed
30 a new strategy to explore phage transformations in the microbial community by direct detection of the
31 temperate viral fragments from metagenome and metavirome. The detectable transformation of
32 temperate phages provided us a new insight into the potential treatment for human disease.
33 Conclusions: DeePhage is the first tool that can rapidly and efficiently identify two kinds of phage
34 fragments especially for metagenomics analysis with satisfactory performance. DeePhage is freely
35 available via <http://cqb.pku.edu.cn/ZhuLab/DeePhage> or <https://github.com/shufangwu/DeePhage>.

36

37 INTRODUCTION

38 In a microbial community, phages are the major component of the viral genetic materials. It is
39 estimated that the number of phages is on average ten times higher than that of bacteria. They may
40 destroy bacteria, meanwhile in some situations benefit populations of bacteria, and thus crucially
41 impact the microbial community [1]. With the development of the high-throughput sequencing
42 technology, a large number of novel phages are discovered from untargeted metagenomes and
43 viromes, in which viral particles are first enriched before sequencing [2,3]. However, the analysis of
44 these phage sequences is a great challenge since the reference genomes of phages are very limited
45 in view of the fact that most of the phages cannot be cultured independently. The complete phage
46 genomes in current databases are much less than that of bacteria, therefore a large number of
47 sequences from virome data cannot find regions with homology to the known phages [2]. In addition,
48 unlike bacteria, phages lack the universal marker genes such as 16S rRNA [4], so that many species
49 identification strategies designed for bacterial analysis are not applicable to phages. Moreover, for
50 mobile elements such as phages, the sequence assembly is often poorer than that of bacteria, usually
51 because the mobile elements carry repetitive regions like insertion sequences and share sequences
52 that occurred among different genomes [5]. As a result, the large number of short fragments in
53 metagenomic data also increases the difficulty of the analysis.

54 To overcome these difficulties, several computational tools focusing on two major tasks have been
55 developed to analyze the phage sequences from metagenome or virome. One of the tasks is to
56 identify phage fragments in untargeted metagenomic data, such as the tools VirSorter [6], VirFinder
57 [7], MARVEL [8], virMine [9], and PPR-Meta [10]. Especially, PPR-Meta is a tool with high
58 performances developed by us and demonstrates much better accuracy than the related tools.

59 Another task is to assign the host for a given phage contig, such as the tools WIsH [11],
60 VirHostMatcher [12], and Hostphinder [13]. However, these tools cannot answer the question about
61 how the discovered phages interact with their hosts. According to the interaction mode, which is also
62 referred to as the phage lifestyle, phages can be divided into the virulent phages and the temperate
63 phages [14]. When a virulent phage infects its host, it will produce many progenies as soon as the
64 phage's DNA is injected into the host cell and then cause the death of the host through bacterial lysis
65 [14]. In contrast, temperate phages can undergo the lysogenic cycle and lytic cycle. In the lysogenic
66 cycle, a temperate phage will integrate its genome into the host chromosome, which is also referred
67 to as prophage, and then copies its genome together with the host chromosome [15]. While induced
68 by appropriate conditions, especially the nutritional conditions and the number of co-infecting phages,
69 temperate phages will go into the lytic cycle, following by releasing the viral particle and killing the
70 host through bacterial lysis [16]. Such different processes have a significant influence on the
71 microbiota especially in the human gut, which could be highly correlated with human diseases or the
72 treatment of human disease. Although some kinds of hotspots, such as phage therapies that making
73 use of the virulent phages in the context of therapeutic use [17], have been investigated, limited by
74 current bioinformatics tools, people still knew little about these different lifecycles for their prevalence
75 in the human gut [18]. Therefore, it is important to distinguish virulent and temperate phages for
76 further understanding of phage-host interaction.

77 Although the classification strategy of this issue for virome data has not been investigated yet,
78 there are several noteworthy works that help to characterize the virulent and temperate phages. Even
79 phages lacking marker genes, those studies show that they may have some functional genes, which
80 are high-frequency genes and can tell us whether a given phage is virulent or temperate in a relatively
81 credible way. For example, Emerson et al. found there were some functional genes for temperate
82 phages, such as integrase and excisionase [19]; Schmidt et al. found that the leucine substitution in
83 DNA *polA* gene had a strong connection with temperate phages [20]. Notably, McNair et al. designed
84 a computational tool called PHACTS to identify whether a phage with a complete or partial proteome
85 is virulent or temperate [14]. This tool employs all the sequence information of proteins from a phage
86 genome and uses the random forest as a classifier to make the judgment. Researchers further found
87 that the existence of some kind of genes helped PHACTS present good results. For example, virulent
88 phages usually have genes related to phage lysis, nucleotide metabolism, or structural proteins, while

89 temperate phages usually contain genes related to toxins, excision, integration, lysogeny, or
90 regulation of expression [14]. Unfortunately, such kind of strategies may not apply to metagenomic
91 data. To date, it is still a difficult task to reconstruct complete genomes of all organisms in the
92 metagenomic data. Therefore, only a few DNA fragments may contain those functional genes that can
93 help to make the judgment. According to the report of PHACTS, this tool can achieve accuracy over
94 95% if at least 25 proteins are provided from a phage genome. However, if fewer proteins are
95 obtained, the accuracy of PHACTS reduces obviously. When only five proteins from a phage,
96 PHACTS only achieves an accuracy of about 65%; if only two proteins from a phage, PHACTS
97 appears to produce random results with an accuracy below 55%. Considering that most of the DNA
98 sequences in metagenomic data are short fragments that only contain a few genes or even
99 incomplete genes, it is essential to develop a tool, which does not depend on using information from
100 sufficient proteins with functional genes level, while to make judgment directly for each short DNA
101 fragment in metagenomic data.

102 In this paper, we present a two-class classifier DeePhage to identify whether a DNA fragment is
103 derived from a virulent phage or a temperate phage. Using the information of every nucleotide without
104 manually feature extracted, DeePhage encodes sequences in “one-hot” form. Such representations
105 are suitable for the Convolutional Neural Network (CNN) model to detect helpful motifs for
106 classification, which are common used on biological sequence identification. Together with other
107 kinds of neural network layers, DeePhage learns different features between virulent and temperate
108 sequences and then outputs a score indicating the possibility to be a certain kind of phage sequence.
109 Tested on the same data, DeePhage can significantly outperform the best of available methods
110 PHACTS on computational efficiency by using only 1/810 computation time that PHACTS uses.
111 Simulation studies on five-fold validation show that DeePhage precedes by approximately 30%
112 compared with PHACTS. DeePhage’s evaluations on real metavirome data of bovine rumen are
113 better than PHACTS with much more accurate results, which use annotations of the BLAST method
114 as a reference. Meanwhile, we present a new strategy to conveniently detect the phage
115 transformation by tracing specific phage contigs, which can explore the influence of phages that
116 contribute to human diseases. DeePhage can be used to analyse the virome data and untargeted
117 metagenomic data directly. While handling the metagenomic data, users need to firstly identify the

118 phage sequences using related software, such as PPR-Meta [10] as we mentioned above, and then
119 use DeePhage to further annotate the phage sequences.

120

121 **MATERIAL AND METHODS**

122 **Data construction**

123 Considering that there is no real virome data with the reliable lifestyle annotation for each sequence
124 as a benchmark, we constructed artificial contigs extracted from well-annotated complete phage
125 genomes as the benchmark to train and test the algorithm. We downloaded 227 complete phage
126 genomes with lifestyle annotations from McNair dataset, including 79 virulent phages and 148
127 temperate phages [14]. Among these phages, we removed two virulent phages from the dataset:
128 mycobacteriophage D29 (accession: NC_001900) and lactococcus lactis bacteriophage ul36
129 (accession: NC_004066), because the lifestyle of these two phages may be ambiguous. Although
130 these two phages are annotated as virulent phages, researchers found that they both contained
131 functional integrases, indicating that they can integrate their genomes into host chromosomes like
132 temperate phages [14]. Besides, D29 is very similar to the temperate phage L5 [21], while ul36 has
133 46.6% homology with the temperate phage Tuc2009 [22]. Therefore, 77 virulent phages and 148
134 temperate ones are used in the current study. In general, the unbalanced size between positive and
135 negative samples may have an impact on the accuracy of the machine learning-based algorithm [7].
136 In the McNair dataset used in this work, it is thus obvious that the number of positive samples is less
137 than that of negative samples. However, we found that the genome length of each positive sample is
138 generally longer than that of each negative sample. It is probably because temperate phages can
139 integrate their genomes into host chromosomes and may discard some non-essential genes. What is
140 more, genes on host chromosomes may be served as compensation. As a result, based on the bases
141 counts, the dataset size between positive samples and negative samples are similar. For
142 convenience, herein the virulent phages are referred to as the positive sample and the temperate
143 phages as the negative sample.

144 We further used MetaSim (v0.9.1) [23] to extract artificial contigs from the complete phage
145 genomes. Considering that the length of contigs in real metagenomes may cover a wide range, we
146 divided the artificial contigs into four groups according to their length: the length range in Group A is
147 100-400 bp; Group B is 400-800 bp; Group C is 800-1200 bp while Group D is 1200-1800 bp. Those

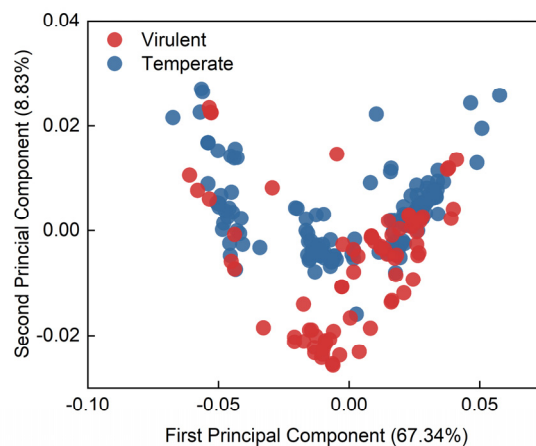
148 four groups may cover the length of raw reads and the average length of assembled contigs from the
149 next-generation sequencing technology. We would evaluate the performance of DeePhage on
150 different groups respectively.

151 We also used real virome data to estimate the reliability of DeePhage qualitatively. We
152 downloaded virome data of bodily fluid in the bovine rumen [24] from MG-RAST [25]. They were
153 downloaded as raw reads (accessions: mgm4534202.3 and mgm4534203.3). We used SPAdes
154 (v3.13.0) [26] to assemble the raw reads and obtained 118918 contigs with the N50 of 291 bp.

155

156 **Mathematical model of phage sequences**

157 To evaluate the feasibility of using sequence signature used for classifying virulent and temperate
158 phages, we first analysed the distribution of k-mer frequencies, which have been widely used to
159 distinguish genomes from different species, among virulent phage genomes and temperate phage
160 genomes. We used 4-mer frequencies to characterize each phage genome in our dataset. The
161 Principal Component Analysis (PCA) [27] revealed that the 4-mer frequencies between virulent and
162 temperate phage genomes have different distribution (Figure 1), showing that they have different
163 sequence signatures to characterize these two categories of phage genomes.



164

165 **Figure 1.** The PCA of 4-mer frequencies distribution among virulent and temperate phage genomes.

166

167 Although k-mer frequencies have shown their ability to classify virulent and temperate phage
168 genomes, using such frequencies to characterize short DNA fragments will usually be disturbed with
169 the noise (11). Also, as global statistics that may miss some local information, k-mer frequencies are
170 difficult to detail characterize mobile elements that contain mosaic structure [28]. To describe the local

171 sequence information in detail, we consider the one-hot encoding form, which can represent every
172 base continuously and entirely. For each sequence, we used the “one-hot” encoding form to represent
173 each base in a sequence. Specifically, bases A, C, G and T were represented by [0,0,0,1], [0,0,1,0],
174 [0,1,0,0], and [1,0,0,0].

175

176 **Algorithm structure of DeePhage**

177 Deep learning algorithms are recognized as an extremely effective method in many fields including in
178 the biology field. Comparing with the Recurrent Neural Network (RNN), the Convolutional Neural
179 Network (CNN) models are faster to train and more efficient in sequential spatial correlations [29].
180 Specifically, CNN is a universal network for extracting local patterns in terms of biology, which in the
181 current context can be used as a motif detector of DNA sequences. In DeePhage, we presented a
182 deep learning algorithm with CNN models to handle the input sequences represented by the one-hot
183 encoding form. The network contained eight layers: a 1D convolutional (Conv1D) layer, one 1D
184 maximum pooling (Maxpooling) layer, one 1D global average pooling (Globalpooling) layer, two batch
185 normalization (BN1 and BN2) layer, a dropout (Dropout) layer, and two dense (Dense1 and Dense2)
186 layers.

187 Conv1D layer takes a sequence encoded by an $L \times 4$ matrix X (L is the length of the sequences,
188 equals 400, 800, 1200, and 1800) as the input and generates total F feature maps as output by
189 corresponding F convolutional kernels. Using ReLU (Rectified Linear Unit) [30] as the activation
190 function, the Conv1D layer output an $L \times F$ matrix Y^C and computes for the f^{th} feature map at the l^{th}
191 location like this:

$$192 \quad Y_{l,f}^C = \text{ReLU}\left(\sum_{m=0}^{M-1} \sum_{n=0}^3 W_{m,n}^f X_{l+m,n} + b_f^C\right),$$

193 for $l = 1, 2, 3, \dots, L - 1$, $f = 1, 2, 3, \dots, F - 1$.

194 The W^f and b_f^C are an $M \times 4$ weight matrix and a bias of the f^{th} kernel. The mentioned ReLU function is
195 defined as [30]:

$$196 \quad \text{ReLU}(x) = \begin{cases} x & \text{if } x \geq 0 \\ 0 & \text{if } x < 0 \end{cases}$$

197 As a traditional nonlinear function, the ReLU function is easier to train and achieves better
198 performance, which can rectify the shortcomings of sigmoid functions. Those kernels scan a

199 sequence one after another to extract the valuable features for the classification and the ReLU
200 function achieves a nonlinear transformation.

201 Such a combination is followed by the Maxpooling layer to downsample the input representation
202 by taking the maximum value over an input channel with a pooling size $S1$ and a stride size $S2$. The
203 window is shifted along with each channel independently and can generate F new channels with the
204 size of L' ($L' = L/S2$). The Maxpooling layer outputs an $L' \times F$ feature matrix Y^M and one of the pooling
205 operation for a specific channel at the l^{th} location defines like this:

$$206 \quad Y_{l,f}^M = \max(Y_{1 \times S2, f}^C, Y_{1 \times S2+1, f}^C, Y_{1 \times S2+2, f}^C, \dots, Y_{1 \times S2+S1-1, f}^C),$$
$$207 \quad \text{for } l = 0, 1, 2, \dots, L' - 1, \quad f = 0, 1, 2, \dots, F - 1,$$

208 Its main function is to reduce the dimensions of each input channel using final summarised features,
209 which can also adapt to location variations of valuable features.

210 Features from the Maxpooling layer are passed to the BN1 layer to scale the inputs. At each
211 batch, it usually transforms inputs to have a mean close to 0 and a standard deviation close to 1,
212 which can avoid the vanishing gradient problem and accelerate the convergence rate of the model.
213 So the output feature matrix Y^{B1} of the BN1 layer is also an $L' \times F$ matrix as Y^M but being scaled.

214 The next is a Dropout layer, which randomly drops a certain proportion (denoted as P) of input
215 elements by setting them to zero during training (29). The output Y^{Dp} is formulated as:

$$216 \quad Y^{Dp} = \mathbf{K} \odot Y^{B1}, \text{ where } \mathbf{K} \sim B(1, P).$$

217 The drop mask \mathbf{K} denotes a Bernoulli distribution with n equals 1 and p equals P . It could effectively
218 reduce overfitting especially in our small dataset [31].

219 After a dropout layer, the Globalpooling layer takes the Y^{Dp} as input and reduce features from the
220 same channel into one dimension by using the average value of those features, which can integrate
221 global spatial information. More formally:

$$222 \quad y_f^G = \frac{1}{L'} \sum_{l=0}^{L'-1} Y_{l,f}^{Dp}, \text{ for } f = 1, 2, 3, \dots, F - 1,$$

223 where y_f^G is the average value of features from the f^{th} input channel. Considering all the F channels
224 from the previous layer, the output of the Globalpooling layer y^G is an F dimension vector.

225 Subsequently, a Dense1 layer using ReLU function as activation function outputs R units. It has
226 an $R \times F$ weight matrix W^{D1} and an R -dimensional bias vector b^{D1} . Each output units is processed by:

227
$$y_r^{D1} = \text{ReLu}(\sum_{f=0}^{F-1} W_{r,f}^{D1} y_f^G + b_r^{D1}), \text{ for } r = 1, 2, 3, \dots, R - 1.$$

228 Dense1 layer can compile the features from different input channels together and finally generate an
229 R-dimensional vector y^{D1} , while a Conv1D layer just extracts features into different feature maps.

230 The vector y^{D1} is then sent into a BN2 layer to generate a new feature vector y^{B2} that having a
231 mean close to 0 and a standard deviation close to 1, which has the same effect as the BN1 layer.

232 Using a sigmoid function as an activation function, the final layer is the Dense2 layer and output
233 only one score between zero and one representing the probability of prediction. Using an R-
234 dimensional weight vector W^{D2} and a bias scalar b^{D2} , the output score is given by:

235
$$y^{D2} = \text{sigmoid}(\sum_{r=0}^{R-1} W_r^{D2} y_r^{B2} + b^{D2}).$$

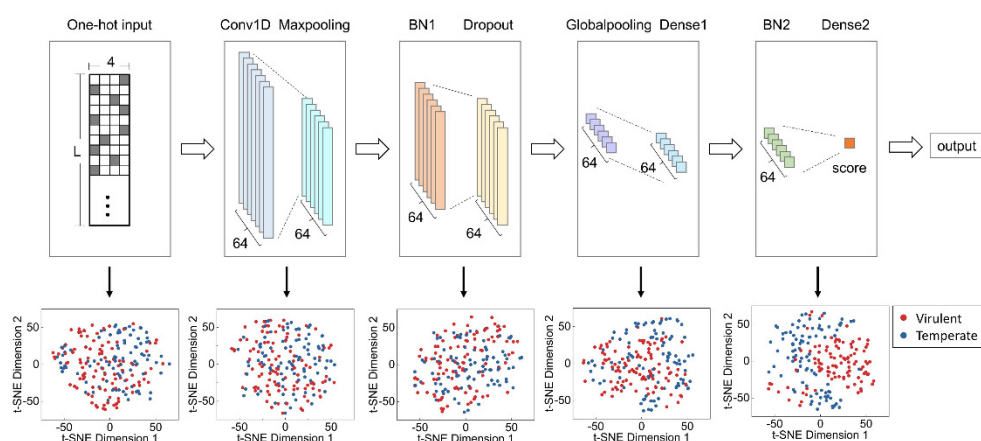
236 The sigmoid function is defined as:

237
$$\text{sigmoid}(x) = \frac{1}{1 + e^{-x}}$$

238 In general, the sequence with a score higher than 0.5 would be regarded as a positive sample (a
239 virulent phage) and the sequence with a score lower than 0.5 would be regarded as a negative
240 sample (a temperate phage). When training, we used the Adam optimizer [32] (learning rate =
241 0.0001), binary cross-entropy as the loss function, and 32 as the batch size to train the neural network
242 and update network weights. Altogether, we found that setting the size F to 64, M to 6, S1 to 3, S2 to
243 3, P to 0.3, and R to 64 made the best performance. The structure of DeePhage was shown in the
244 upper part of Figure 2.

245 It is worthy to know more about the importance of the encoding method for sequences and each
246 specific layer in our model, so we tested six different models (including DeePhage) by using k-mer
247 frequencies as an encoding representation or removing a certain layer. The six model architectures
248 (DeePhage, Kmer-4, No-Maxpooling, No-Dropout, No-Globalpooling, and No-BN) were shown in
249 Additional File 1 (Figure S1) and their performances were shown in Additional File 1 (Table S1). It can
250 be seen that the Kmer-4 model did a terrible prediction. As mentioned above, when we used 4-mer
251 frequencies to characterize each phage at the level of genome sequences (as shown in Figure 1), it
252 could slightly distinguish two kinds of phages. It is proved that k-mer frequencies have not enough
253 power to represent short sequences and are fit for capturing the global signature of long sequences
254 rather than the local signature of short sequences. As for those models removing a certain layer, the

255 performance dropped compared with DeePhage. Especially, the prediction accuracy reduced nearly
256 10% and 5% when using a model without a Globalpooling layer and BN layers (No-Globalpooling and
257 No-BN model). Other models decreased slightly. We can see the architecture and the one-hot
258 encoding representation of DeePhage are better than others.



259 Note: Conv1D, 1D convolutional layer; Maxpooling, 1D maximum pooling layer; Globalpooling, 1D global average pooling layer; BN1, first batch
260 normalization layer; BN2, second batch normalization layer; Dropout, dropout layer; Dense1, first dense layer; Dense2, second dense layer
261

262 **Figure 2.** Structure of deep learning neural network and visualization of five layers by reducing dimensions. DeePhage uses
263 the Convolutional Neural Network as the classifier. The neural network (in the upper part) takes the sequence in the “one-hot”
264 coding form as input and output a score between zero and one. In general, the sequence with a score higher than 0.5 can be
265 referred to as the virulent phage-derived fragment and the sequence with a score lower than 0.5 can be referred to as the
266 temperate phage-derived fragment. The visualization demonstrated the learning process of DeePhage. The performance would
267 be better when we observing a deeper layer (in the lower part).

268 Although deep neural networks are considered as black-box models, we hope to have insights
269 about the learning process for features. We chose five layers (One-hot input, Conv1D, BN1,
270 Globalpooling, and BN2) to observe their learned features. Because it is hard to gain an intuitive
271 feeling about high-dimension features, we used t-Distributed Stochastic Neighbor Embedding (t-SNE)
272 [33], which is a machine learning algorithm for dimensionality reduction, for the visualization of high-
273 dimensional data in a 2D projected space. During the training period, we firstly used PCA to reduce
274 features into a 20-dimensional space and then used t-SNE to reduce them into a two-dimensional
275 space using the sequences from Group D. The visualizations of five layers were shown in the lower
276 part of Figure 2. It could be seen that the effects of classification are better when focusing on the
277 deeper layers. In detail, two types of phages were firstly mixture together and then separated
278 gradually, which demonstrated the learning process of DeePhage. Furthermore, it should be

279 emphasized that the visualizations by dimensionality reduction cannot reflect the complete power of
280 DeePhage.

281 Considering the other length of sequences beyond our four-trained groups, we design some
282 strategies. For those sequences longer than 1800 bp, DeePhage will split the sequence into several
283 1800-bp-long subsequences without overlapping, usually except the last subsequence. DeePhage will
284 then use the neural network in the corresponding group to predict each subsequence, and calculate
285 the weighted average score according to the score and length of each subsequence. Because
286 training the neural network using long sequences is very time-consuming, we do not train additional
287 neural networks for longer sequences. For those sequences shorter than 100 bp, DeePhage uses the
288 neural network in Group A to predict.

289

290 **RESULTS**

291 **Identification performance of DeePhage**

292 We first used the five-fold cross validation to evaluate the performance of DeePhage. To test whether
293 DeePhage can distinguish the lifestyle of novel phages or not, for each validation, we divided the
294 training set and the test set based on complete genomes rather than artificial contigs, and then
295 simulated 20,000 training sequences and 20,000 test ones using MetaSim [23]. The performance
296 evaluation criteria here are defined as: $S_n = TP / (TP + FN)$; $S_p = TN / (TN + FP)$; and $Acc = (TP + TN) / (TP +$
297 $TN + FN + FP)$. Among these criteria, S_n and S_p are used to evaluate the accuracy of virulent phages
298 and temperate phages respectively, while Acc is used to evaluate the overall performance. As shown
299 in Table 1, DeePhage demonstrates overall reliable and stable performance with Acc from 75% to
300 88%. Such results indicate that the input of functional genes with several proteins is not required for
301 our DeePhage. Therefore, our DeePhage method shows an evident advantage compared with the
302 tool PHACTS. Since DeePhage can identify each DNA fragment as the virulent phage-derived
303 sequence or temperate phage-derived one directly and independently, it would be a more acceptable
304 tool to analyse phages in metagenomic data. In this case, the complete or near-complete genomes
305 for phages were hard to be reconstructed from the data, especially for those with low abundance or in
306 a low coverage sequencing condition. Clearly, our DeePhage has the advantage of being applicable
307 to processing the data by current short-read sequencing technologies and performs better when the
308 short reads could be assembled into longer contigs.

309 **Table 1.** Results of five-fold cross-validation for DeePhage. The validation of each group was performed independently. Each
310 result consists of the mean and standard deviation.

Group	Group A (100-400 bp)	Group B (400-800 bp)	Group C (800-1200 bp)	Group D (1200-1800 bp)
<i>Sn</i> (%)	69.3±3.6	76.2±5.5	82.1±6.6	86.9±4.7
<i>Sp</i> (%)	78.8±5.8	86.1±6.9	88.6±9.6	88.7±8.9
<i>Acc</i> (%)	74.6±1.9	81.8±2.7	85.8±4.0	88.2±4.3

311

312 It is noted that the *Sn* is slightly lower than *Sp* for each rotation of different length groups, which
313 means that some virulent phage-derived sequences are more prone to be misjudged as temperate
314 ones. The reason is possibly that the diversity of virulent phages is lower than that of temperate
315 phages in the current database. Although the sizes of positive and negative samples are comparable
316 based on base counts, the number of genomes in positive samples is less than that of negative
317 samples. In general, sequences from the same genome have similar sequence signatures such as
318 codon usage and GC content. The fewer number of genomes in positive samples may lead to lower
319 diversity. From the algorithm of machine learning, the negative samples have a wider distribution in
320 the feature space while the positive samples only occupy a smaller space. Therefore, for the test
321 data, the positive samples are easier to fall out of their feature space, which leads to the misjudgment
322 of DeePhage. Despite this, the performance of DeePhage on virulent phages is rather reliable. More
323 details about the performances of the ROC curves and AUC scores of DeePhage in each rotation of
324 the five-fold cross validation are shown in Additional File 1 (Figure S2).

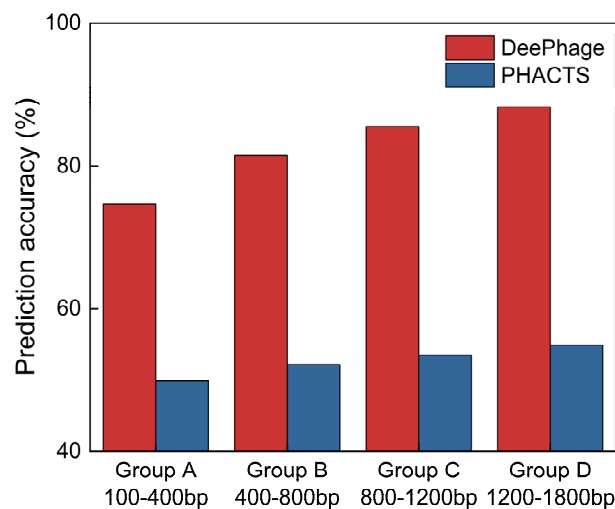
325 In general, sequences with scores near 0.5 are not as reliable as those sequences with a score
326 near 0 or 1. Therefore, DeePhage is designed with an adjustable cutoff to filter out these uncertain
327 predictions. Users can specify a cutoff using a parameter. In this way, a sequence with a score
328 between $(0.5 - \text{cutoff}/2, 0.5 + \text{cutoff}/2)$ will be labelled as "uncertain". In general, with a higher cutoff, the
329 percentage of uncertain predictions will be higher while the remaining predictions will be more
330 reliable.

331

332 **Comparison with PHACTS for protein sequence identification**

333 It should be noted that DeePhage and PHACTS were designed for different tasks, PHACTS was
334 designed for complete genomes while DeePhage is designed for metagenomic fragments. Therefore,
335 the requirements of the input data for them are actually different. PHACTS requires users to input all
336 proteins (amino acid sequences) within one phage genome, so proteins from different phages should

337 not be put into the same file. In contrast, the DeePhage's requirement is only to input all DNA
338 fragments (nucleic acid sequences), no matter whether they contain coding regions and whether they
339 are from the same phage, and DeePhage may directly judge each fragment independently. Although
340 it is difficult to compare two tools based on the same condition, we tried to test the performance of
341 PHACTS in DNA short fragments. Since PHACTS requires a collection of protein sequences as input,
342 we firstly annotated the protein sequences of 100,000 DNA sequences of the test set in each length
343 group using FragGeneScan (v1.31) [34] and proteins from the same sequence (sequences without
344 coding regions were ignored) are input into the program PHACTS (v0.3). As for comparison,
345 DeePhage is also used to predict these DNA sequences with coding regions. The total accuracy (the
346 number of correct predictions divided by the total number of sequences having the coding regions in
347 each length group) of DeePhage and PHACTS in each length group are shown in Figure 3. For short
348 fragments covering data sets of Group A to D, PHACTS demonstrates the accuracies of ACC around
349 50%, which are nearly the results of random predictions. In construct, DeePhage can satisfactorily
350 classify the sequences with the accuracies of ACC about 75%~88%.



351

352 **Figure 3.** Comparison results of DeePhage and PHACTS in each length group.

353

354 In addition, we have evaluated the performances of DeePhage and PHACTS on the coding
355 sequences (CDSs) from all 225 phage genomes. Since PHACTS could only process protein
356 sequences, we extracted all CDSs from the genomes according to the GenBank annotation and each
357 CDS was independently inputted to PHACTS (in the form of amino acid sequences) and DeePhage

358 (in the form of nucleic acid sequences). We found that PHACTS can only achieve the *Acc* of 54.3%,
359 which is also similar to random judgment results, while DeePhage achieves the *Acc* of 85.0%, more
360 than 30% higher than that of PHACTS. Considering that the number of CDSs in each metagenomic
361 fragment is very limited, PHACTS has actually a very limited ability to analyse metagenomic data
362 especially when the complete genomes could not be reconstructed using these fragments. Overall, as
363 the first tool designed for phage lifestyle classification from metagenomic data, DeePhage, a de novo
364 tool using the deep learning algorithm, presents efficient prediction.

365 Also, DeePhage can handle large scale high-throughput data within an acceptable running time.
366 In order to test, we recorded the runtime of DeePhage and PHACTS to predict 100 DNA sequences
367 (converted to protein sequences for PHACTS) ranging from 100-1800 bp. DeePhage spends nearly
368 10 seconds 810 times faster than PHACTS using nearly 135 minutes, when tested on a virtual
369 machine with the following configuration: CPU: Intel Core i7 4790; and Memory: 8G, DDR3. As for
370 PHACTS, every sequence needs to be aligned and every prediction needs to be replicated ten times,
371 while DeePhage could directly predict every sequence without any alignments. Therefore, DeePhage
372 is much faster than PHACTS.

373

374 **Evaluation of DeePhage and PHACTS using real metavirome data**

375 Although it was difficult to make exact evaluations using real data, some functional genes could help
376 us to make an approximately effective assessment of our model. In this subsection, we used
377 DeePhage to predict all the sequences in a metavirome data of bovine rumen [24] with 118918
378 contigs assembled by SPAdes (v3.13.0) [26]. As a result, 45.1% (53625/118918) of the contigs were
379 predicted as virulent phage-derived contigs and 54.9% (65293/118918) as temperate phage-derived
380 contigs. For assessment of the DeePhage's prediction, we then collected the RefSeq viral protein
381 database [35] as a reference. Since the viral proteins labelled of 'excision', 'integration', or 'lysogeny'
382 are more likely to exist in temperate phages [14], we used those proteins to build an MTPD (mini
383 temperate phage-derived) set containing 107 protein sequences. We then searched all 118918
384 contigs against the MTPD data using Blastx v2.7.1[36] and obtained 16 targeted contigs having
385 homologous regions ($e\text{-value} \leq 1e-10$, hits length ≥ 400). Those presented an extremely small
386 proportion (16/118918), which confirms that there are a huge number of data having no reliable
387 homologous regions of known databases. When it comes to DeePhage, 13 of 16 targeted contigs can

388 be identified as temperate phage-derived contigs, while only 10 contigs can be classified as
 389 temperate phage-like contigs by PHACTS. It shows DeePhage performs better than PHACTS and
 390 has rather the potential to analyze newly sequenced phage data. However, the prediction scores
 391 being nearly 0.5 shows PHACTS actually made randomly inferring, while DeePhage having a majority
 392 of reliable scores and making better predictions. The information of 16 targeted contigs and predicted
 393 results by DeePhage and PHACTS was listed in Table 2.

394

395 **Table 2.** Information of 16 targeted contigs and predicted results by DeePhage and PHACTS. ‘Contig ID’ refers
 396 to the ID of 16 targeted contigs. ‘Identity’, ‘E-value’, and ‘Hits length’ refer to the alignment results using Blastx.

Contig ID	Contig length (bp)	Identity (%)	E-value	Hits length	DeePhage		PHACTS	
					prediction	score	prediction	score
4	28516	26.32	1e-10	513	temperate	0.4308	temperate	0.4835
12	11212	27.23	2e-14	606	temperate	0.2022	temperate	0.4667
52	5349	29.89	1e-30	798	temperate	0.0127	temperate	0.4995
88	3734	24.68	1e-11	828	temperate	0.1326	temperate	0.4925
173	2530	26.22	2e-25	1044	temperate	0.0232	virulent	0.5000
223	2233	23.27	1e-12	834	virulent	0.6742	virulent	0.5161
1257	1029	29.87	1e-16	462	virulent	0.6044	virulent	0.5082
1639	921	23.96	2e-11	849	temperate	0.1589	temperate	0.4735
3299	702	28.18	8e-25	609	temperate	0.0303	temperate	0.4744
3326	699	30.88	9e-15	405	temperate	0.3095	virulent	0.5055
6405	549	25.14	1e-13	519	temperate	0.0222	virulent	0.5080
7704	514	39.86	2e-22	429	temperate	0.1451	virulent	0.5110
8130	503	36.05	3e-22	441	temperate	0.0512	temperate	0.4944
9804	470	31.69	2e-16	423	temperate	0.1596	temperate	0.4952
10819	454	38.61	2e-30	450	temperate	0.0574	temperate	0.4951
12636	430	34.04	2e-21	417	virulent	0.9784	temperate	0.4743

397

398 Further, we found that 16 contigs contain homologous regions of the functional proteins with the
 399 e-value lower than 1e-10, but they do not have high identity scores to these proteins (identity<50%).
 400 These results indicate that the 16 contigs are not close to the viral proteins from the database in the
 401 genetic relationship. These also show that the diversity of phages in the environmental samples might
 402 be much higher than that in the current database, and DeePhage can handle these novel phages. In
 403 fact, when we looked over the RefSeq viral protein database, we found that a large number of
 404 proteins are labelled as putative or hypothetical and the percentage of such proteins might be much
 405 higher than that of bacteria, which further demonstrates the diversity of phages.

406 Not only the several above-mentioned contigs but also the whole sequences could be taken into
407 consideration in a full scope of the predictive ability of DeePhage. Using the whole genomes of 77
408 virulent and 148 temperate phages in our datasets, we annotated all the sequences in the virome
409 data of bovine rumen by Blastn v2.7.1[36]. When setting the default parameters (the default e-value is
410 10), 118564 contigs could be annotated as virulent or temperate phage genomes by BLAST. Among
411 those contigs, DeePhage distinguished 49.32% virulent and 57.69% temperate phage contigs with an
412 average proportion of 54.4%. In comparison, PHACTS made an apparent preference for virulent
413 contigs (68.2%) and for temperate contigs (28.9%). Although the proportion of virulent contigs was
414 higher, PHACTS only received an average of 44.5%, which was much lower than DeePhage.
415 Estimated on the level of entire real data, the superiority of DeePhage is certainly considerable.

416 To sum up, the evaluation of DeePhage using real metavirome data demonstrated DeePhage
417 made much better and reliable predictions than PHACTS. As an ab initial tool, it may be concluded
418 that DeePhage has a good ability to adapt to this diversity and has the potential to analyse newly
419 sequenced phage data.

420

421 **An application of a cross-sectional study indicating that phage transformations impacting the** 422 **change of gut microbiota structure**

423 Viruses especially the phages contribute importantly to the gut microbiota structure. Particularly,
424 temperate phages could be free from the genome of their bacterial hosts and then kill them driven by
425 a suitable environment condition. While virulent phages directly attack their host. Therefore, such
426 phage transformations would change the gut microbiota composition profile and community structure.
427 However, it is hard to analyse this result entirely using the databased method because of the
428 limitation of database and marker genes like 16S RNA. As a result, there are not effectively
429 computational related tools. For example, alignment phage sequences to the known phage database
430 using the traditional Blast program could just output some known phages without any new phages.
431 Indeed, the number of unknown phages were extraordinarily huge. Fortunately, DeePhage now could
432 detect phage transformations over the whole genomes of phages from the complete virome data. The
433 downstream findings based on DeePhage could give us instructive insights into the function of
434 phages in the gut microbiota.

435 In this subsection, we then designed a new strategy about how to use DeePhage to estimate the
436 transformations of phages in the cross-sectional study. Specially, we analyse the virome data from
437 ulcerative colitis (UC) patients and healthy people as an example to find out associations between
438 phages and gut microbiota after having the disease. For phages in a community, owing to lack of
439 marker genes like 16S RNA to detect their abundance or diversity, it is difficult to determine the
440 association between the transformation of phages and the change of gut microbiota structure. Herein
441 we collected 21 untargeted metagenomic samples (randomly selected) of UC patient guts and 21
442 (randomly selected) untargeted metagenomic samples of healthy human guts by Nielsen et al. [37]. In
443 addition, we collected 54 virome samples (viral particles were enriched before sequencing) of UC
444 patient guts (being diagnosed as a specific state) and 23 virome samples of healthy control by
445 Norman et al. [38]. The accessions were provided in Additional File 1 (Table S1 and S2). We used
446 SPAdes to assemble raw reads of each sample.

447 For each untargeted metagenomic sample, we first used PPR-Meta [10] to identify all the phage-
448 derived contigs. The average percentage of phage contigs in metagenomic data of UC patient and
449 healthy individual guts were similar (23.7% in UC patient and 25.7% in healthy human guts) without
450 significant difference (p -value=0.170, the difference in location=0.021 and 95% confidence interval =
451 (-0.007, 0.045) for two-sided Wilcoxon Rank-Sum test). For convenience, in the following text, phage
452 contigs in gut microbiota annotated by PPR-Meta were referred to as computational phages while
453 contigs from virome data were referred to as experimental phages. It was worth noting that
454 experimental phages only included virulent phages and temperate phages in the lytic cycle. However,
455 temperate phages in the lysogenic cycle could not be included, because temperate phages in the
456 lysogenic cycle would integrate their genomes into host cells and would not assemble the viral
457 particles. In contrast, computational phages included all kinds of phages.

458 We then used DeePhage to predict the lifestyle of the experimental phages. An average of 64.2%
459 of the contigs were predicted as temperate phages in UC patients while 51.5% in healthy individuals
460 with significant difference (p -value=0.001, difference in location=0.123 and 95% confidence interval =
461 (0.054, 0.200) for two-sided Wilcoxon Rank-Sum test). This indicates that the proportion of temperate
462 phages in UC patients' gut was higher than in healthy individuals. However, we still could not infer the
463 detailed transformations from this result, because both the decreased diversity of virulent phages and
464 increased diversity of temperate phages in UC patients will lead to a higher proportion of temperate

465 phages. More importantly, even if the number of virulent phages and temperate phages were the
466 same in healthy individuals and UC patients, the proportion of temperate phages in experimental
467 phages could also increase when more temperate phages were undergoing the transformation from
468 the lysogenic cycle to the lytic cycle, in which they would assemble free viral particles. To make the
469 population dynamics clearer, we further used DeePhage to predict the lifestyle of the computational
470 phages. Surprisingly, an average of 57.5% and 56.9% of the contigs were predicted as temperate
471 phages in UC patients and healthy individuals without significant difference (p -value=0.811, the
472 difference in location=-0.003 and 95% confidence interval = (-0.036, 0.025) for two-sided Wilcoxon
473 Rank-Sum test), indicating that the proportion of virulent phages and temperate phages in UC
474 patients and healthy individuals were similar. Considering the results from computational phages and
475 experimental phages together, it seemed that the higher proportion of temperate phages in
476 experimental phages of UC patients might result from the part of temperate phages undergoing a
477 transformation from the lysogenic cycle to the lytic cycle.

478 From these preliminary results, we inferred that the phage populations in UC patients were
479 undergoing a kind of change that influence the gut microbiota structure, in which some kinds of
480 temperate phages were transforming from prophages to free viral particles. To investigate the
481 transforming temperate phages, we picked out all the temperate contigs annotated by DeePhage from
482 the UC and healthy samples. Using all the phage genomes [39] as the database of the BLAST
483 method (e -value $\leq 1e-10$), 342 species of phages were existing in both Healthy and UC samples, and
484 just 154 species, 99% of which were from the *Caudovirales* order, only existing in Healthy samples.
485 As a comparison, we found out different phage contigs coming from 551 species that only existing in
486 UC samples, which probably means there were more kinds of temperate phages in UC samples than
487 in Healthy samples. Those phages could be classified into eleven families: *Siphoviridae*,
488 *Herelleviridae*, *Podoviridae*, *Myoviridae*, *Ackermannviridae*, *Autographiviridae*, *Drexelviriidae*,
489 *Tristromaviridae*, *Inoviridae*, *Microviridae*, *Sphaerolipoviridae*. The first seven families belong to the
490 *Caudovirales* order, which accounts for nearly 97% (532/551) different species. Besides, a very small
491 part (nine different species) is coming from *Microviridae* family. *Caudovirales* order and *Microviridae*
492 family are dominated in human gut virome [40], meanwhile, they are more abundant in UC patients
493 compared with household members and controls [41]. Especially, Norman et al. observed an increase
494 in the richness of some members of the *Caudovirales* in UC patients [38]. Those supported our

495 inference to a certain degree. The last several families lacking researchers' concerns in the human
496 gut could roughly be ignored. Since the release of prophages is often associated with the death of
497 bacterial hosts, the activation of the temperate phages may be associated with the change of species
498 composition. We can infer that after being illness more kinds of temperate *Caudovirales* phages turn
499 into a lytic cycle and become free viral particles from the bacterial genomes, in consequence, such
500 switch change the struct of microbiota by killing the bacterial host. Consistently, previous research
501 showed that the species compositions of the bacteria community in UC patients were different from
502 that of healthy individuals [42] and the virulent phages from the healthy core could be substituted by
503 temperate phages [43]. All those discoveries indicated that maybe it was the temperate *Caudovirales*
504 phages have a primary impact on human UC disease, which was also verified by us. However,
505 DeePhage could not only detect well-studied phages, such as *Caudovirales* phages, but it also can
506 trace any known and unknown phages to distinguish their lifestyles. With integrated data, we have
507 access to disease conditions deeply.

508 To sum up, such a strategy being independent of databases may further provide insights into the
509 specific and integral interactions between phages and bacterial hosts according to phage lifestyles,
510 which could not have been found out before. Researchers can gain more valuable information about
511 the disease process and facilitate the study of human disease.

512

513 **DISCUSSION**

514 In this paper, we presented DeePhage as an effective tool to distinguish virulent phage-derived and
515 temperate phage-derived sequences in metavirome data. Coding a DNA sequence, DeePhage needs
516 no previously extracted features but use each nucleotide as input. There are some advantages.
517 DeePhage can bypass using the information of some functional genes to make the judgment and
518 directly and rapidly identify each DNA fragment being independent of assembling. Such a function is
519 important because many novel phage genomes are difficult to reconstruct and the amount of
520 sequences is large when focused on metagenomic data. CNN models here occupied the core
521 strength of DeePhage for their excellent ability on feature extraction, which is hard to discover by
522 statistics. As we can see, DeePhage gradually separates virulent and temperate phage-derived
523 sequences along with deeper neural networks. DeePhage's ability to distinguish two kinds of
524 sequences is superior to PHACTS on the assessment of simulated data and real data. To be specific,

525 DeePhage presents a huge improvement in prediction accuracy (nearly 30% higher on simulated
526 data) and computational efficiency (almost 810 times faster). More importantly, DeePhage sheds new
527 light on the phage transformations by tracing the variation of a specific type of phage. As we can see,
528 the previous study speculated the possibility that the expansion of the *Caudovirales* phages is related
529 to the activation of prophages in UC patients [44]. Fortunately, now we can be more convinced that
530 more temperate *Caudovirales* phages are turning into a lytic cycle. We believe that there will be an
531 increasing number of new discoveries, just like the problem mentioned before, on account of
532 DeePhage. Afterward, DeePhage ultimately reduces the dependency on culture-dependent methods
533 and promotes human disease research.

534 It is also interesting to explore the biological mechanism that helps DeePhage distinguish
535 fragments from these two kinds of phage using the sequence signature. In our opinion, this may
536 because virulent phages and temperate phages face different evolutionary pressures and therefore
537 contain different sequence signatures, such as k-mer frequencies as we showed in Figure 1. Genome
538 amelioration often occurs on foreign DNA, such as phage or plasmid, in the host cell and foreign DNA
539 will change its sequence signatures according to the host chromosome to help it exist stably in the
540 host cell [45]. The similarity of sequence signatures between foreign DNA and bacterial chromosome
541 is often used to predict the bacterial host of the foreign DNA [11,12,45]. Since temperate phages will
542 spend more time in the host cell, they may adjust their sequence signatures toward host
543 chromosomes. Related researches also show that temperate phages do contain more similar
544 sequence signatures to their hosts than virulent phages [21,46]. Therefore, we considered that the
545 difference of sequence signatures played an important role for DeePhage to identify these two kinds
546 of phages. To further prove this conjecture, we collected 120 bacterial genomes from RefSeq
547 database [47] (the accession numbers can be seen in Additional File1, Table S4) and then used
548 MetaSim to extract artificial contigs between 100 to 1800 bp. We observed how DeePhage would
549 judge these bacterial sequences. Although the training set of DeePhage did not contain any bacterial
550 sequences, DeePhage identified 79.3%, 84.7%, 84.9%, and 86.0% of the bacterial sequences as
551 temperate phages in Group A, B, C, and D, respectively (the sequence length in each group was
552 corresponding to Table 1). We considered that the reason why more than half of the bacterial
553 sequences were identified as temperate phages was that bacteria contained similar sequence

554 signatures with temperate phages. This phenomenon also demonstrates that using the information of
555 sequence signatures may be the working principle of DeePhage.

556 DeePhage also has some limitations. Although prokaryotic viruses are dominant in virome
557 samples, a few eukaryotic viruses could also be included. However, DeePhage cannot identify these
558 sequences before distinguishing the lifestyle of each contig. Fortunately, the related tool that helps to
559 distinguish prokaryotic and eukaryotic viruses has been developed recently [48] and we are also
560 considering constructing a preprocessing module for DeePhage to filter out the eukaryotic viruses so
561 that DeePhage can generate more reliable results for the downstream analysis.

562 In conclusion, to the best of our knowledge, DeePhage is the first tool that can directly judge
563 each fragment as a virulent phage-derived or temperate phage-derived sequence for virome data in a
564 fast way. Therefore, it is expected that DeePhage will be a powerful tool for researchers who are
565 interested in the function of phage populations and phage-host interactions.

566

567 **Availability of supporting data and materials**

568 The artificial contigs, related scripts, and original results are available at
569 <http://cqb.pku.edu.cn/ZhuLab/DeePhage/data/>. All the other data are available at corresponding
570 references mentioned in the main text.

571 **Availability of supporting source code and requirements**

572 Project name: DeePhage.

573 Project home page: <http://cqb.pku.edu.cn/ZhuLab/DeePhage> or
574 <https://github.com/shufangwu/DeePhage>.

575 Operating system: The code of DeePhage was written on Linux. We optimized the program in a
576 virtual machine; thus, DeePhage is platform independent.

577 Programming language: python, matlab

578 Other requirements: no other requirements are needed if running in the virtual machine. If not, Python
579 3.6.7, TensorFlow 1.4.0, Keras 2.1.3, numpy 1.16.4, h5py 2.9.0 and MATLAB Component Runtime
580 2018a (for free) are needed. MATLAB is not necessary.

581 License: GPL-3.0.

582 RRID: SCR_019243

583

584 **Additional files**

585 Additional file 1: Figure S1. The architectures of six different models; Table S1. The Sn, Sp, and Acc
586 of six different models; Figure S2. The ROC curves and AUC scores of DeePhage performances in
587 each set of five-fold cross-validation; Table S2. The accession numbers of 21 untargeted
588 metagenomic samples of the healthy human gut and 21 untargeted metagenomic samples of UC
589 patients' gut; Table S3. The accession numbers of 23 virome samples of the healthy human gut and
590 54 virome samples of UC patients' gut; Table S4. The accession numbers of 120 bacterial genomes
591 from RefSeq database.

592

593 **Authors' contributions**

594 H.Q.Z. and S.F.W. proposed and designed the study. J.T. constructed the datasets. S.F.W. and
595 Z.C.F. optimized the code. M.L., C.H.W., and Q.G. contributed to the analysis. C.M.X and X.Q.J
596 helped to test the results. S.F.W. and H.Q.Z. wrote and revised the manuscript, and all authors
597 proofread and improved the manuscript.

598

599 **ACKNOWLEDGEMENT**

600 We thank Dr. Li Qu, Luotong Wang, Man Zhou and Chuan He of Peking University for their helpful
601 discussions. Part of the analysis was performed on the High Performance Computing Platform of the
602 Center for Life Science of Peking University.

603

604 **FUNDING**

605 This work was supported by the National Key Research and Development Program of China
606 (2017YFC1200205) and the National Natural Science Foundation of China (32070667, 31671366).

607

608 **CONFLICT OF INTEREST**

609 The authors declare that they have no competing interests.

610

611 **TABLE AND FIGURES LEGENDS**

612 **Figure 1.** The PCA of 4-mer frequencies distribution among virulent and temperate phage genomes.

613 **Figure 2.** Structure of deep learning neural network and visualization of five layers by reducing
614 dimensions. DeePhage uses the Convolutional Neural Network as the classifier. The neural network
615 (in the upper part) takes the sequence in the “one-hot” coding form as input and output a score
616 between zero and one. In general, the sequence with a score higher than 0.5 can be referred to as
617 the virulent phage-derived fragment and the sequence with a score lower than 0.5 can be referred to
618 as the temperate phage-derived fragment. The visualization demonstrated the learning process of
619 DeePhage. The performance would be better when we observing a deeper layer (in the lower part).

620 **Table 1.** Results of five-fold cross-validation for DeePhage. The validation of each group was
621 performed independently. Each result consists of the mean and standard deviation.

622 **Figure 3.** Comparison results of DeePhage and PHACTS in each length group.

623 **Table 2.** Information of 16 targeted contigs and predicted results by DeePhage and PHACTS. ‘Contig
624 ID’ refers to the ID of 16 targeted contigs. ‘Identity’, ‘E-value’, and ‘Hits length’ refer to the alignment
625 results using Blastx.

626

627 REFERENCES

- 628 1. Wommack, K.E. and Colwell, R.R. Virioplankton: Viruses in aquatic ecosystems. *Microbiol. Mol.*
629 *Biol. Rev.* 2000;**64**(1):69-114.
- 630 2. Hayes, S., Mahony, J., Nauta, A. and van Sinderen, D. Metagenomic Approaches to Assess
631 Bacteriophages in Various Environmental Niches. *Viruses* 2017;**9**(6):127.
- 632 3. Paez-Espino, D., Eloë-Fadrosh, E.A., Pavlopoulos, G.A., Thomas, A.D., Huntemann, M.,
633 Mikhailova, N., Rubin, E., Ivanova, N.N. and Kyrpides, N.C. Uncovering Earth's virome. *Nature*
634 2016;**536**(7617):425-430.
- 635 4. Mokili, J.L., Rohwer, F. and Dutilh, B.E. Metagenomics and future perspectives in virus discovery.
636 *Curr Opin Virol.* 2012;**2**(1):63-77.
- 637 5. Rozov, R., Kav, A.B., Bogumil, D., Shterzer, N., Halperin, E., Mizrahi, I. and Shamir, R. Recycler:
638 an algorithm for detecting plasmids from de novo assembly graphs. *Bioinformatics*
639 2017;**33**(4):475-482.
- 640 6. Roux, S., Enault, F., Hurwitz, B.L. and Sullivan, M.B. VirSorter: mining viral signal from microbial
641 genomic data. *Peerj* 2015;**3**:e985.

- 642 7. Ren, J., Ahlgren, N.A., Lu, Y.Y., Fuhrman, J.A. and Sun, F.Z. VirFinder: a novel k-mer based tool
643 for identifying viral sequences from assembled metagenomic data. *Microbiome* 2017;**5**(1):69.
- 644 8. Amgarten, D., Braga, L.P.P., da Silva, A.M. and Setubal, J.C. MARVEL, a Tool for Prediction of
645 Bacteriophage Sequences in Metagenomic Bins. *Front Genet.* 2018;**9**:304.
- 646 9. Garretto, A., Hatzopoulos, T. and Putonti, C. virMine: automated detection of viral sequences from
647 complex metagenomic samples. *Peerj* 2019;**7**:e6695.
- 648 10. Fang, Z.C., Tan, J., Wu, S.F., Li, M., Xu, C.M., Xie, Z.J. and Zhu, H.Q. PPR-Meta: a tool for
649 identifying phages and plasmids from metagenomic fragments using deep learning. *Gigascience*
650 2019;**8**(6):giz066.
- 651 11. Galiez, C., Siebert, M., Enault, F., Vincent, J. and Soding, J. WIsH: who is the host? Predicting
652 prokaryotic hosts from metagenomic phage contigs. *Bioinformatics* 2017;**33**(19):3113-3114.
- 653 12. Ahlgren, N.A., Ren, J., Lu, Y.Y., Fuhrman, J.A. and Sun, F.Z. Alignment-free d(2)(*)
654 oligonucleotide frequency dissimilarity measure improves prediction of hosts from
655 metagenomically-derived viral sequences. *Nucleic Acids Res.* 2017;**45**(1):39-53.
- 656 13. Villarroel, J., Kleinheinz, K.A., Jurtz, V.I., Zschach, H., Lund, O., Nielsen, M. and Larsen, M.V.
657 HostPhinder: A Phage Host Prediction Tool. *Viruses* 2016;**8**(5):116.
- 658 14. McNair, K., Bailey, B.A. and Edwards, R.A. PHACTS, a computational approach to classifying the
659 lifestyle of phages. *Bioinformatics* 2012;**28**(5):614-618.
- 660 15. Mirzaei, M.K. and Maurice, C.F. Menage a trois in the human gut: interactions between host,
661 bacteria and phages. *Nat Rev Microbiol.* 2017;**15**(7):397-408.
- 662 16. Erez, Z., Steinberger-Levy, I., Shamir, M., Doron, S., Stokar-Avihail, A., Peleg, Y., Melamed, S.,
663 Leavitt, A., Savidor, A., Albeck, S. *et al.* Communication between viruses guides lysis-lysogeny
664 decisions. *Nature* 2017;**541**(7638):488-493.
- 665 17. Brives, C. and Pourraz, J. Phage therapy as a potential solution in the fight against AMR:
666 obstacles and possible futures. *Palgrave Commun.* 2020;**6**:100.
- 667 18. Sutton, T.D.S. and Hill, C. Gut Bacteriophage: Current Understanding and Challenges. *Front*
668 *Endocrinol (Lausanne).* 2019;**10**:784.
- 669 19. Emerson, J.B., Thomas, B.C., Andrade, K., Allen, E.E., Heidelberg, K.B. and Banfield, J.F.
670 Dynamic Viral Populations in Hypersaline Systems as Revealed by Metagenomic Assembly. *Appl*
671 *Environ Microbiol.* 2012;**78**(17):6309-6320.

- 672 20. Schmidt, H.F., Sakowski, E.G., Williamson, S.J., Polson, S.W. and Wommack, K.E. Shotgun
673 metagenomics indicates novel family A DNA polymerases predominate within marine
674 viroplankton. *ISME J.* 2014;**8**(1):103-114.
- 675 21. Deschavanne, P., Dubow, M.S. and Regeard, C. The use of genomic signature distance between
676 bacteriophages and their hosts displays evolutionary relationships and phage growth cycle
677 determination. *Virology*. 2010;**7**:163.
- 678 22. Labrie, S. and Moineau, S. Complete genomic sequence of bacteriophage u136: Demonstration
679 of phage heterogeneity within the P335 quasi-species of lactococcal phages. *Virology*
680 2002;**296**(2):308-320.
- 681 23. Richter, D.C., Ott, F., Auch, A.F., Schmid, R. and Huson, D.H. MetaSim-A Sequencing Simulator
682 for Genomics and Metagenomics. *Plos One* 2008;**3**(10):e3373.
- 683 24. Ross, E.M., Petrovski, S., Moate, P.J. and Hayes, B.J. Metagenomics of rumen bacteriophage
684 from thirteen lactating dairy cattle. *BMC Microbiol.* 2013;**13**:242.
- 685 25. Meyer, F., Paarmann, D., D'Souza, M., Olson, R., Glass, E.M., Kubal, M., Paczian, T., Rodriguez,
686 A., Stevens, R., Wilke, A. *et al.* The metagenomics RAST server - a public resource for the
687 automatic phylogenetic and functional analysis of metagenomes. *Bmc Bioinformatics* 2008;**9**:386.
- 688 26. Bankevich, A., Nurk, S., Antipov, D., Gurevich, A.A., Dvorkin, M., Kulikov, A.S., Lesin, V.M.,
689 Nikolenko, S.I., Pham, S., Pribelski, A.D. *et al.* SPAdes: A New Genome Assembly Algorithm and
690 Its Applications to Single-Cell Sequencing. *J Comput Biol.* 2012;**19**(5):455-477.
- 691 27. Wold, S., Esbensen, K. and Geladi, P. Principal Component Analysis. *Chemometr Intell Lab Syst*
692 1987;**2**(1-3):37-52.
- 693 28. Ford, M.E., Sarkis, G.J., Belanger, A.E., Hendrix, R.W. and Hatfull, G.F. Genome structure of
694 mycobacteriophage D29: Implications for phage evolution. *J Mol Biol.* 1998;**279**(1):143-164.
- 695 29. Zheng, D.D., Pang, G.S., Liu, B., Chen, L.H. and Yang, J. Learning transferable deep
696 convolutional neural networks for the classification of bacterial virulence factors. *Bioinformatics*
697 2020;**36**(12):3693-3702.
- 698 30. Agarap, A.F. Deep Learning using Rectified Linear Units (ReLU). *arXiv.* 2018.
699 <https://arxiv.org/abs/1803.08375>
- 700 31. Srivastava, N., Hinton, G., Krizhevsky, A., Sutskever, I. and Salakhutdinov, R. Dropout: A Simple
701 Way to Prevent Neural Networks from Overfitting. *J. Mach. Learn. Res.* 2014;**15**(1):1929-1958.

- 702 32. Kingma, D. and Ba, J. Adam: a method for stochastic optimization. arXiv. 2014.
703 <https://arxiv.org/abs/1412.6980v8>
- 704 33. van der Maaten, L. and Hinton, G. Visualizing Data using t-SNE. J. Mach. Learn. Res.
705 2008;**9**:2579-2605.
- 706 34. Rho, M.N., Tang, H.X. and Ye, Y.Z. FragGeneScan: predicting genes in short and error-prone
707 reads. Nucleic Acids Res. 2010;**38**(20):e191.
- 708 35. The NCBI database. <ftp://ftp.ncbi.nih.gov/refseq/release/viral/>. Accessed 6 June 2018
- 709 36. Johnson, M., Zaretskaya, I., Raytselis, Y., Merezhuk, Y., McGinnis, S. and Madden, T.L.
710 NCBI BLAST: a better web interface. Nucleic Acids Res. 2008;**36**:W5-W9.
- 711 37. Nielsen, H.B., Almeida, M., Juncker, A.S., Rasmussen, S., Li, J.H., Sunagawa, S., Plichta, D.R.,
712 Gautier, L., Pedersen, A.G., Le Chatelier, E. *et al.* Identification and assembly of genomes and
713 genetic elements in complex metagenomic samples without using reference genomes. Nat
714 Biotechnol. 2014;**32**(8):822-828.
- 715 38. Norman, J.M., Handley, S.A., Baldrige, M.T., Droit, L., Liu, C.Y., Keller, B.C., Kambal, A.,
716 Monaco, C.L., Zhao, G., Fleshner, P. *et al.* Disease-Specific Alterations in the Enteric Virome in
717 Inflammatory Bowel Disease. Cell 2015;**160**(3):447-460.
- 718 39. The NCBI database. ftp://ftp.ncbi.nlm.nih.gov/genomes/GENOME_REPORTS/. Accessed 23
719 November 2020
- 720 40. Sutton, T.D.S. and Hill, C. Gut Bacteriophage: Current Understanding and Challenges. Front
721 Endocrinol (Lausanne) 2019;**10**:784.
- 722 41. Scarpellini, E., Ianiro, G., Attili, F., Bassanelli, C., De Santis, A. and Gasbarrini, A. The human gut
723 microbiota and virome: Potential therapeutic implications. Dig Liver Dis. 2015;**47**(12):1007-1012.
- 724 42. Qin, J.J., Li, R.Q., Raes, J., Arumugam, M., Burgdorf, K.S., Manichanh, C., Nielsen, T., Pons, N.,
725 Levenez, F., Yamada, T. *et al.* A human gut microbial gene catalogue established by
726 metagenomic sequencing. Nature 2010;**464**(7285):59-65.
- 727 43. Clooney, A.G., Sutton, T.D.S., Shkoporov, A.N., Holohan, R.K., Daly, K.M., O'Regan, O., Ryan,
728 F.J., Draper, L.A., Plevy, S.E., Ross, R.P. *et al.* Whole-Virome Analysis Sheds Light on Viral Dark
729 Matter in Inflammatory Bowel Disease. Cell Host Microbe 2019;**26**(6):764-778.e765.
- 730 44. Mukhopadhy, I., Segal, J.P., Carding, S.R., Hart, A.L. and Hold, G.L. The gut virome: the 'missing
731 link' between gut bacteria and host immunity? 2019. doi: 10.1177/1756284819836620

- 732 45. Suzuki, H., Yano, H., Brown, C.J. and Top, E.M. Predicting Plasmid Promiscuity Based on
733 Genomic Signature. *J Bacteriol.* 2010;**192**(22):6045-6055.
- 734 46. Ahmed, S., Saito, A., Suzuki, M., Nemoto, N. and Nishigaki, K. Host-parasite relations of bacteria
735 and phages can be unveiled by Oligostickiness, a measure of relaxed sequence similarity.
736 *Bioinformatics* 2009;**25**(5):563-570.
- 737 47. Pruitt, K.D., Tatusova, T. and Maglott, D.R. NCBI Reference Sequence (RefSeq): a curated non-
738 redundant sequence database of genomes, transcripts and proteins. *Nucleic Acids Res.*
739 2005;**33**:D501-D504.
- 740 48. Galan, W., Bak, M. and Jakubowska, M. Host Taxon Predictor - A Tool for Predicting Taxon of the
741 Host of a Newly Discovered Virus. *Sci Rep.* 2019;**9**(1):3436.
742